

Codeword-Segmentation Rate-Splitting Multiple Access and Evaluation under Suboptimal Decoding

Sibo Zhang, *Graduate Student Member, IEEE*, Bruno Clerckx, *Fellow, IEEE*, David Vargas

Abstract—Rate-Splitting Multiple Access (RSMA) has been recognized as a promising multiple access technique. We propose a novel architecture for downlink RSMA, namely Codeword-Segmentation RSMA (CS-RSMA). Different from conventional RSMA which splits users' messages into common and private parts before encoding, CS-RSMA encodes the users' messages directly, segments the codewords into common and private parts, and transmits the codeword segments using common and private streams. In addition to the principle of CS-RSMA, a novel performance analysis framework is proposed. This framework utilizes a recent discovery in mismatched decoding under finite-alphabet input and interference, and can better capture the receiver's complexity limits. Precoder optimization under finite alphabets and suboptimal decoders for conventional RSMA and CS-RSMA to maximize the Sum-Rate (SR) and the Max-Min Fairness (MMF) is also addressed. The numerical results reveal the theoretical performance of conventional RSMA and CS-RSMA. We observe that CS-RSMA leads to better performance than conventional RSMA in SR, and similar performance in MMF. Furthermore, a physical-layer implementation of CS-RSMA is proposed and evaluated through link-level simulations. Aside performance benefits, we also demonstrate that CS-RSMA brings significant benefits on the encoding/decoding, control signaling, and retransmission process compared to conventional RSMA.

Index Terms—Rate-splitting multiple access (RSMA), multi-antenna broadcast channel, finite-alphabet signalling, mismatched decoding, bit-interleaved coded modulation.

I. INTRODUCTION

Emerging wireless networks, such as 6G, face increasing demands for high spectral efficiency and user fairness in massive connectivity. Such demands require the development of advanced multiple access techniques [1], [2]. Rate-Splitting Multiple Access (RSMA) has arisen as a promising paradigm due to its numerous advantages in terms of efficiency, reliability, robustness, low latency, flexibility and universality [3]. The key idea of downlink RSMA involves combining part of users' messages into common streams, which are transmitted in a multicast fashion, whereas the rest of messages are transmitted through private streams in a unicast fashion. The existence of a mixture of common and private streams provides flexibility

and improved interference management capability compared to conventional techniques, such as Orthogonal Multiple Access (OMA), Space-Division Multiple Access (SDMA) and Non-Orthogonal Multiple Access (NOMA), as demonstrated theoretically and numerically [3], and experimentally [4].

In the majority of the existing work on RSMA, Successive Interference Cancellation (SIC) is assumed to be implemented at the receivers to separate common and private streams. More recently, [5] considers RSMA under finite alphabets and proposed non-SIC receivers for RSMA and the corresponding transmitter design, also called SIC-free RSMA¹. Although most prior works analyze RSMA under Gaussian-distributed inputs, the analysis and evaluation of RSMA under finite alphabets are motivated by two factors: (1) most practical systems operate with finite alphabets due to the ease on hardware requirement and encoding/decoding; (2) finite-alphabet interference is less detrimental than Gaussian-distributed interference, it is therefore possible to preserve the benefit of having a mixture of common and private streams without removing the common streams. In [5], SIC-free RSMA has been shown to lead to savings in receiver complexity and latency, but only with a minor sacrifice in both theoretical performance, measured by constellation-constrained mutual information, and practical performance, measured by Link-Level Simulations (LLS). [6], [7] further propose precoder optimization for SIC-based and SIC-free RSMA under finite alphabets. The results verified that RSMA's advantage is preserved under finite alphabets, and that SIC-free RSMA leads to only minor loss compared to RSMA with SIC.

SDMA is currently the predominant spatial domain technique in use. Despite the numerous benefits of RSMA from theoretical analysis, replacing SDMA with RSMA in practical systems will introduce several challenges. Although the SIC-free receiver designs proposed in [5] addressed the increase in receiver complexity, other challenges remain. These include:

- Increased encoding/decoding complexity: with RSMA, more codewords are transmitted (especially with multi-layer schemes such as the hierarchical RSMA in [8] and the general framework of multi-layer RSMA in [9]), which leads to more complexity in encoding and decoding.
- Control signaling overhead: The increased number of streams requires an increased control signaling overhead to assist in decoding at receivers.

¹Previous studies use the terms "non-SIC" and "SIC-free" interchangeably, as they convey the same meaning.

This work was supported in part by the UK Engineering and Physical Sciences Research Council, Industrial Case award number 210163.

S. Zhang is with the Department of Electrical and Electronic Engineering at Imperial College London, London SW7 2AZ, UK and BBC Research and Development, The Lighthouse, White City Place, 201 Wood Lane, London, W12 7TQ, U.K. (e-mail: sibozhang19@imperial.ac.uk).

B. Clerckx is with the Department of Electrical and Electronic Engineering at Imperial College London, London SW7 2AZ, UK (e-mail: b.clerckx@imperial.ac.uk).

D. Vargas is with BBC Research and Development, The Lighthouse, White City Place, 201 Wood Lane, London, W12 7TQ, U.K. (e-mail: david.vargas@bbc.co.uk).

- **Retransmission:** As the common stream is intended for multiple users, it requires retransmission mechanisms that are different from SDMA, such as in [10]. The design of an efficient retransmission process for RSMA schemes poses a challenge.

Another direction that deserves exploration is to evaluate and design RSMA schemes using performance metrics that account for more practical limitations. The benefit of RSMA has been well studied under Gaussian input signals, for example in [8], [9], [11] and [12]. The evaluation of achievable rates under finite block lengths is studied in [13], [14]. The achievable rates under finite-alphabet input constraints are studied in [5]–[7].

The above works consider performance metrics originating from the mutual information, which is proved to be achievable with reliable communications by Shannon’s channel coding theorem [15]. The proofs of the channel coding theorem assume optimal decoding, for example, the joint typicality decoding in [15] and the maximum-likelihood decoding in [16]. However, optimal decoding is often difficult in practice due to limited channel knowledge and/or complexity reasons. Therefore, it is interesting to discover achievable rates under suboptimal decoders, leading to the study of mismatched decoding [17]–[19]. A recent work [20] studies communication in finite-alphabet input channels under Gaussian noise and finite-alphabet interference, where the decoders fully or partially approximate the interference as Gaussian random variables to reduce computational complexity, namely Finite-Alphabet Gaussian Channel under Interference (FAGCI). This model reflects a common issue that interference is not properly detected in receivers for complexity reasons. A lower bound on the mismatched capacity is derived using the Generalized Mutual Information (GMI).

In this work, a novel downlink RSMA architecture is proposed, namely Codeword-Segmentation RSMA (CS-RSMA), to reduce implementation challenges of RSMA. The contribution of this work is summarized as follows:

- We propose a novel downlink architecture for RSMA, namely CS-RSMA. Unlike conventional RSMA which splits users’ messages into common and private parts, then combined the common parts into a common message before encoding, CS-RSMA encodes users’ messages directly, segments the resulting codewords into common and private parts, and combine the common parts into a common stream. Details on encoding and decoding procedures for both conventional RSMA and CS-RSMA are provided.
- We apply the GMI derived in [20] to analyze the achievable rate of CS-RSMA and conventional RSMA to capture receiver imperfection in practice. This leads to a different analysis from [7] where the achievable rate is measured by mutual information, which can only be achieved by optimal decoders, e.g., the maximum likelihood decoder. With the GMI, conventional RSMA and CS-RSMA can be evaluated under the assumption that the decoders treat undesired private streams as Gaussian random variables, despite the fact that they are from finite

alphabets. Such suboptimal decoders reveal the performance of commonly used low-complexity receivers that treat interference as Gaussian noise instead of demodulating them, as demonstrated in [20]. To ensure a fair comparison, a decoding complexity constraint is defined.

- To reveal the theoretical performance of conventional RSMA and CS-RSMA, we develop precoder optimization methods to maximize Sum-Rate (SR) and Max-Min Fairness (MMF) among users, under the assumption of finite alphabets and suboptimal decoders. To exploit the flexibility of RSMA, we allow adaptive alphabet selection under a decoding complexity constraint. Numerical results from the proposed optimization algorithms are provided, which shows that CS-RSMA outperforms conventional RSMA with and without SIC in terms of SR and performs similarly to the two in terms of MMF.
- While the achievable rate given by GMI measures theoretical limits and provides closed-form expressions for system design, they are based on idealized signal-space encoding and decoding, which remain to be a challenge in practice. Although the achievable rate of a proper channel model reflects the throughput in practical systems, more accurate evaluation can be obtained through LLS that involves practical designs, i.e., those incorporating binary encoding/decoding and modulation. For this purpose as well as improving the practicality of CS-RSMA, we propose physical-layer (PHY) transceiver designs for CS-RSMA, and apply LLS to measure the Bit Error Rate (BER) performance of the proposed designs. Similarly to the achievable rate results, the LLS results show that CS-RSMA slightly outperforms conventional RSMA. From the perspective of practical applications, the benefits of CS-RSMA over conventional RSMA are also discussed in terms of encoding/decoding complexity, control signalling overhead, and retransmission design.

Organization: The rest of this paper is organized as follows. In Section II, we introduce the system model for both conventional RSMA and CS-RSMA. In Section III, results from [20] on multi-user communications with suboptimal decoders are briefly summarized. This then leads to the performance metric of conventional RSMA and CS-RSMA to be considered in this work, as well as a definition of decoding complexity. In Section IV, to evaluate the theoretical performance of conventional RSMA and CS-RSMA, SR and MMF optimization methods that capture the suboptimal decoders are proposed. Section V summarizes the numerical results on the theoretical performance. In Section VI, we propose the PHY implementation of CS-RSMA and evaluate it using LLS, and discuss the implementation benefits of CS-RSMA over conventional RSMA. Finally, Section VII concludes this paper.

Notations: Scalars are denoted by normal letters. Sequences and vectors are denoted by bold letters. Random variables are denoted by capital letters, while the specific values are denoted by lower case letters. For example, x is an observation of X , and \mathbf{x} is an observation of \mathbf{X} . Multisets are denoted by calligraphic letters. $P(\cdot)$ and $P_{\cdot|\cdot}(\cdot|\cdot)$ denote probability and conditional probability respectively. \mathbf{I} and $\mathbf{0}$ denotes the iden-

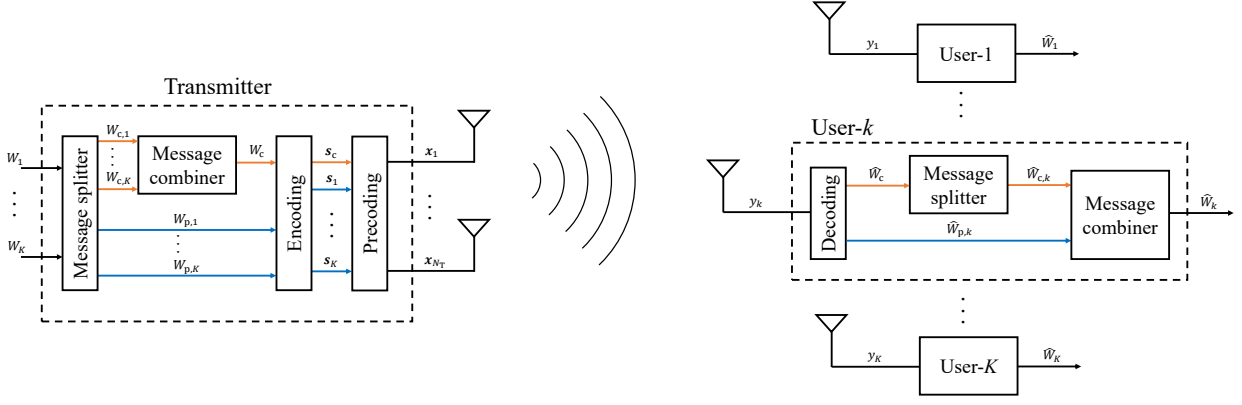


Fig. 1. Conventional RSMA for multi-user MISO.

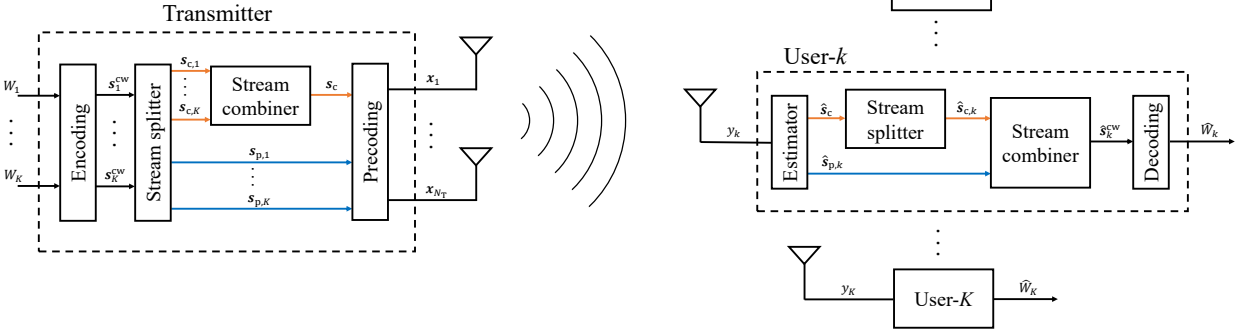


Fig. 2. Codeword-Segmentation RSMA for multi-user MISO.

tivity matrix and the zero matrix, whose dimensions are given by their superscripts. $[\cdot]_{m,n}$ denotes the (m,n) -th entry of a matrix. $(\cdot)^T$, $(\cdot)^H$, $\|\cdot\|$ and $\|\cdot\|_F$ denote respectively the transpose, conjugate transpose, Euclidean norm and Frobenius norm of the input entity. $|\cdot|$ denotes the absolute value if the argument is a scalar, or the cardinality if the argument is a set. \times denotes the Cartesian product of two sets. $\mathbb{E}[\cdot]$ denotes the expectation. $\mathcal{CN}(\mu, \Sigma)$ denotes circular symmetric complex Gaussian distribution for vectors whose mean and covariance matrix are μ and Σ . $\dim(\cdot)$ denotes the dimension of the argument.

II. CODEWORD SEGMENTATION RSMA

We consider a downlink multi-user Multiple-Input Single-Output (MISO) system where a transmitter equipped with N_T transmit antennas serves K users with unicast messages, $\{W_1, \dots, W_K\}$. We assume narrow-band channels and let n denote the transmission block length. At time instant $t \in \{1, 2, \dots, n\}$, the received signal at user- k , $k \in \mathcal{K} = \{1, \dots, K\}$, can be written as

$$y_{t,k} = \mathbf{h}_k^H \mathbf{x}_t + z_{t,k}, \quad (1)$$

where \mathbf{x}_t is the transmitted signal, \mathbf{h}_k is the channel between the transmitter and user- k and $z_{t,k} \sim \mathcal{CN}(0, \sigma_z^2)$ is the additive white Gaussian noise observed by user- k . We assume that the transmitter applies single-layer RSMA [9], [11], hence the transmit signal can be expressed as

$$\mathbf{x}_t = \mathbf{P} \mathbf{s}_t, \quad (2)$$

where $\mathbf{P} = [\mathbf{p}_c, \mathbf{p}_{p,1}, \dots, \mathbf{p}_{p,K}] \in \mathbb{C}^{N_T \times (K+1)}$ represents the precoding matrix and $\mathbf{s}_t = [s_{t,c}, s_{t,p,1}, \dots, s_{t,p,K}]^T \in \mathbb{C}^{(K+1) \times 1}$ represents the transmitted symbol vector. We assume $\mathbb{E}\{\mathbf{s}_t \mathbf{s}_t^H\} = \mathbf{I}$, and the transmission is subject to a power budget P_T , where $P_T = \mathbb{E}\{\mathbf{x}_t^H \mathbf{x}_t\} = \|\mathbf{P}\|_F^2$. A collection of symbol vectors at all the time instances can be written as $\mathbf{S} = [\mathbf{s}_1, \mathbf{s}_2, \dots, \mathbf{s}_n] \in \mathbb{C}^{(K+1) \times n}$. The rows of \mathbf{S} are $K+1$ symbol blocks (streams), resulting in an alternative expression, $\mathbf{S} = [\mathbf{s}_c, \mathbf{s}_{p,1}, \dots, \mathbf{s}_{p,K}]^T$, where \mathbf{s}_c and $\mathbf{s}_{p,k}$, $\forall k \in \mathcal{K}$, are referred to as common and private streams in RSMA. We assume that the symbols in \mathbf{s}_c and $\mathbf{s}_{p,k}$, $\forall k \in \mathcal{K}$, are uniformly drawn from their corresponding alphabets, denoted by \mathcal{X}_c and $\mathcal{X}_{p,k}$.

The general procedures for encoding $\{W_1, \dots, W_K\}$ into $\{\mathbf{s}_c, \mathbf{s}_{p,1}, \dots, \mathbf{s}_{p,K}\}$ at the transmitter and decoding them in the receivers differ in conventional RSMA and the proposed CS-RSMA. Both are described below and are depicted in Fig. 1 and 2, without constraining the specific code and the decoding algorithm in use.

- 1) *Conventional RSMA*: $\{W_1, \dots, W_K\}$ are first split into common and private parts, $\{W_{c,1}, \dots, W_{c,K}\}$ and $\{W_{p,1}, \dots, W_{p,K}\}$, respectively. The common parts are combined into one common message, W_c , while the private parts remain separate as private messages. The $K+1$ messages, $\{W_c, W_{p,1}, \dots, W_{p,K}\}$, are then encoded into $K+1$ codewords, $\{\mathbf{s}_c, \mathbf{s}_{p,1}, \dots, \mathbf{s}_{p,K}\} \subset \mathbb{C}^{n \times 1}$. Upon reception, user- k decodes the received signal into estimates of W_c and $W_{p,k}$, denoted by \hat{W}_c and

$\widehat{W}_{p,k}$. It then extracts from \widehat{W}_c an estimate of its desired common part, denoted by $\widehat{W}_{c,k}$. Finally, user- k combines $\widehat{W}_{c,k}$ and $\widehat{W}_{p,k}$ to obtain an estimate of the desired unicast message, denoted by \widehat{W}_k .

- 2) *Codeword-Segmentation RSMA*: We introduce CS-RSMA as a novel alternative implementation to conventional RSMA. In CS-RSMA, $\{W_1, \dots, W_K\}$ are first encoded into K codewords, $\{s_1^{cw}, \dots, s_K^{cw}\}$, where $s_k^{cw} \in \mathbb{C}^{n_k \times 1}$, $\forall k \in \mathcal{K}$, and n_k is the codeword length for user- k satisfying the following constraint:

$$\sum_{k=1}^K n_k = (K+1)n. \quad (3)$$

$\{s_1^{cw}, \dots, s_K^{cw}\}$ are then segmented into private and common parts. The private parts have a uniform length n and are denoted by $\{s_{p,1}, \dots, s_{p,K}\} \subset \mathbb{C}^{n \times 1}$. The common parts are denoted by $\{s_{c,1}, \dots, s_{c,K}\}$, where $s_{c,k} \in \mathbb{C}^{(n_k-n) \times 1}$, $\forall k \in \mathcal{K}$. The common parts are then combined (e.g., concatenated or interleaved) into one symbol stream, denoted by s_c , and the private parts remain as separate private streams. As a consequence of (3), $s_c \in \mathbb{C}^{n \times 1}$. Upon reception, user- k estimates s_c and $s_{p,k}$ from y_k and output \widehat{s}_c and $\widehat{s}_{p,k}$. Then it extracts an estimate of its desired codeword segment from \widehat{s}_c , denoted by $\widehat{s}_{c,k}$. $\widehat{s}_{c,k}$ and $\widehat{s}_{p,k}$ are combined into \widehat{s}_k^{cw} , an estimate of s_k^{cw} . Finally, based on \widehat{s}_k^{cw} , user- k decodes its desired message, \widehat{W}_k .

The main difference between conventional RSMA and CS-RSMA lies in the order of encoding and splitting: at the transmitter, conventional RSMA splits the messages before encoding them, whereas CS-RSMA directly encodes the messages and segments the codewords; at the receivers, the conventional RSMA decodes the common and private streams before reconstructing the message, whereas CS-RSMA first reconstructs the desired codeword from the codeword segments, and then decodes the reconstructed codeword into the desired message.

Regarding receiver implementation, SIC can be implemented with conventional RSMA. With SIC receivers, each user can first decode the common message, re-encode it into an estimate of the common stream, remove/cancel the estimated common stream from the received signal, and decode the desired private message. Meanwhile, SIC-free receivers provide a low-complexity option for conventional RSMA [5], where re-encoding and cancellation are not performed. With CS-RSMA, SIC cannot be implemented. This is because the common stream is not a codeword, but a combination of segmented codewords from different users, and therefore cannot be decoded directly. SIC-free receivers are still valid for CS-RSMA. Fortunately, [7] shows that SIC-free receivers only incur a minor performance loss in RSMA compared to SIC receivers. Therefore, the absence of SIC in the CS-RSMA is not a critical limitation.

III. PERFORMANCE EVALUATION USING MISMATCHED DECODING

In [5]–[7], the performance of SIC-based and SIC-free receivers is studied considering constellation-constrained

mutual information. However, mutual information has only been shown to be achievable under the assumption of optimal decoding (e.g., the maximum likelihood decoding in [16]). Optimal decoders can be computationally prohibitive when the number of signals observed by the receivers increases. Recently, [20] investigated a channel model that takes finite-alphabet input and is disrupted by finite-alphabet interference and Gaussian noise, namely the FAGCI model. Under the FAGCI model, [20] considers suboptimal decoders that treat part of finite-alphabet interference as Gaussian random variables and derives the GMI as a performance metric under such suboptimal decoders. Strong connections between suboptimal decoders and demodulators are also depicted in [20], making the GMI for the FAGCI model an accurate physical layer abstraction for formulating signal processing problems. Extension to a multiple-antenna setup is also discussed.

In this section, we first summarize the results on the GMI for the FAGCI model under MISO scenarios from [20]. Then, to address scenarios where complexity constraints are imposed on receivers, we apply the GMI to analyze and evaluate the performance of conventional RSMA and CS-RSMA.

A. GMI for Finite Alphabet Input Gaussian Channel Under Interference

A generic expression for the received signal at user- k , $\forall k \in \{1, \dots, K\}$, can be written as follows:

$$y_{t,k} = \mathbf{h}_k^H (\mathbf{p}_x x_{t,k} + \mathbf{P}_i \mathbf{i}_t + \mathbf{P}_j \mathbf{j}_t) + z_{t,k}. \quad (4)$$

$x_{t,k}$, \mathbf{i}_t and \mathbf{j}_t are respectively the desired symbol for user- k , the interfering symbol vector to be treated optimally and the interfering symbol vector to be treated as Gaussian random variables by user- k , respectively drawn from \mathcal{X} , \mathcal{I} and \mathcal{J} with uniform distribution. \mathbf{p}_x , \mathbf{P}_i and \mathbf{P}_j are respectively the precoders for x_t , \mathbf{i}_t and \mathbf{j}_t . $z_{t,k}$ is additive noise generated from the i.i.d. $\mathcal{CN}(0, \sigma_z^2)$. Without loss of generality, we assume that $\mathbb{E}[|x|^2] = 1$, $\mathbb{E}[\mathbf{i}\mathbf{i}^H] = \mathbf{I}^{\dim(\mathbf{i})}$ and $\mathbb{E}[\mathbf{j}\mathbf{j}^H] = \mathbf{I}^{\dim(\mathbf{j})}$ unless any of the alphabets is $\{0\}$, i.e., no signal is transmitted. The decoder at user- k can be written as

$$\hat{m} = \arg \max_{m=1, \dots, M} q^n(\mathbf{x}_k^{(m)}, \mathbf{y}_k), \quad (5)$$

where M is the size of the codebook, $\mathbf{x}_k^{(m)}$ is the m -th codeword, and \mathbf{y}_k is the output sequence. Due to the memoryless nature of (4), the following decomposition can be made:

$$q^n(\mathbf{x}_k^{(m)}, \mathbf{y}_k) = \prod_{t=1}^n q(x_{t,k}^{(m)}, y_{t,k}). \quad (6)$$

The optimal (matched) decoding metric is given by

$$q(x, y) = \sum_{\bar{\mathbf{i}} \in \mathcal{I}} \sum_{\bar{\mathbf{j}} \in \mathcal{J}} \exp \left(- \frac{|y - \mathbf{h}_k^H \mathbf{P}_i \bar{\mathbf{i}} - \mathbf{h}_k^H \mathbf{P}_j \bar{\mathbf{j}} - \mathbf{h}_k^H \mathbf{p}_x x|^2}{\sigma_z^2} \right). \quad (7)$$

With fixed precoders, (7) achieves the matched capacity of (4), which is given by mutual information under finite-alphabet constraints.

It can be observed that the complexity of (7) depends on the cardinality of $\bar{\mathbf{i}}$ and $\bar{\mathbf{j}}$, which can be significant as the number of

$$\begin{aligned}
& I_{\text{GMI},k}(\mathbf{h}_k^H \mathbf{p}_x \mathcal{X}, \mathbf{h}_k^H \mathbf{P}_i \mathcal{I}, \mathbf{h}_k^H \mathbf{P}_j \mathcal{J}, \sigma_z^2) \\
&= \sup_{s \geq 0} \log |\mathcal{X}| - \frac{1}{|\mathcal{X}| |\mathcal{I}| |\mathcal{J}|} \sum_{x \in \mathcal{X}} \sum_{\mathbf{i} \in \mathcal{I}} \sum_{\mathbf{j} \in \mathcal{J}} \mathbb{E}_Z \left[\log \sum_{\bar{x} \in \mathcal{X}} \left(\sum_{\bar{\mathbf{i}} \in \mathcal{I}} \exp \left(- \frac{|\mathbf{h}_k^H \mathbf{p}_x (x - \bar{x}) + \mathbf{h}_k^H \mathbf{P}_i (\mathbf{i} - \bar{\mathbf{i}}) + \mathbf{h}_k^H \mathbf{P}_j \mathbf{j} + n|^2}{\|\mathbf{h}_k^H \mathbf{P}_j\|^2 + \sigma_z^2} \right) \right)^s \right] \\
&+ \frac{1}{|\mathcal{I}| |\mathcal{J}|} \sum_{\mathbf{i} \in \mathcal{I}} \sum_{\mathbf{j} \in \mathcal{J}} \mathbb{E}_Z \left[\log \left(\sum_{\bar{\mathbf{i}} \in \mathcal{I}} \exp \left(- \frac{|\mathbf{h}_k^H \mathbf{P}_i (\mathbf{i} - \bar{\mathbf{i}}) + \mathbf{h}_k^H \mathbf{P}_j \mathbf{j} + n|^2}{\|\mathbf{h}_k^H \mathbf{P}_j\|^2 + \sigma_z^2} \right) \right)^s \right] \quad (9)
\end{aligned}$$

$$\begin{aligned}
& I_{\text{GMI},k}^{\text{approx}}(\mathbf{h}_k^H \mathbf{p}_x \mathcal{X}, \mathbf{h}_k^H \mathbf{P}_i \mathcal{I}, \mathbf{h}_k^H \mathbf{P}_j \mathcal{J}, \sigma_z^2) \\
&= \log |\mathcal{X}| - \frac{1}{|\mathcal{X}| |\mathcal{I}| |\mathcal{J}|} \sum_{x \in \mathcal{X}} \sum_{\mathbf{i} \in \mathcal{I}} \sum_{\mathbf{j} \in \mathcal{J}} \log \sum_{\bar{x} \in \mathcal{X}} \sum_{\bar{\mathbf{i}} \in \mathcal{I}} \exp \left(- \frac{|\mathbf{h}_k^H \mathbf{p}_x (x - \bar{x}) + \mathbf{h}_k^H \mathbf{P}_i (\mathbf{i} - \bar{\mathbf{i}}) + \mathbf{h}_k^H \mathbf{P}_j \mathbf{j}|^2}{\|\mathbf{h}_k^H \mathbf{P}_j\|^2 + 2\sigma_z^2} \right) \\
&+ \frac{1}{|\mathcal{I}| |\mathcal{J}|} \sum_{\mathbf{i} \in \mathcal{I}} \sum_{\mathbf{j} \in \mathcal{J}} \log \sum_{\bar{\mathbf{i}} \in \mathcal{I}} \exp \left(- \frac{|\mathbf{h}_k^H \mathbf{P}_i (\mathbf{i} - \bar{\mathbf{i}}) + \mathbf{h}_k^H \mathbf{P}_j \mathbf{j}|^2}{\|\mathbf{h}_k^H \mathbf{P}_j\|^2 + 2\sigma_z^2} \right) \quad (10)
\end{aligned}$$

$$\begin{aligned}
& \nabla_{\tilde{\mathbf{P}}_k} I_{\text{GMI},k}^{\text{approx}}(\mathbf{h}_k^H \mathbf{p}_x \mathcal{X}, \mathbf{h}_k^H \mathbf{P}_i \mathcal{I}, \mathbf{h}_k^H \mathbf{P}_j \mathcal{J}, \sigma_z^2) \\
&= - \frac{1}{|\mathcal{X}| |\mathcal{I}| |\mathcal{J}|} \sum_{x \in \mathcal{X}} \sum_{\mathbf{i} \in \mathcal{I}} \sum_{\mathbf{j} \in \mathcal{J}} \frac{1}{\sum_{\bar{x} \in \mathcal{X}} \sum_{\bar{\mathbf{i}} \in \mathcal{I}} g(\tilde{\mathbf{P}}_k, \mathbf{v})} \sum_{\bar{x} \in \mathcal{X}} \sum_{\bar{\mathbf{i}} \in \mathcal{I}} g_1(\tilde{\mathbf{P}}_k, \mathbf{v}) + \frac{1}{|\mathcal{I}| |\mathcal{J}|} \sum_{\mathbf{i} \in \mathcal{I}} \sum_{\mathbf{j} \in \mathcal{J}} \frac{1}{\sum_{\bar{\mathbf{i}} \in \mathcal{I}} h(\tilde{\mathbf{P}}_k, \mathbf{w})} \sum_{\bar{\mathbf{i}} \in \mathcal{I}} h_1(\tilde{\mathbf{P}}_k, \mathbf{w}) \quad (11)
\end{aligned}$$

$$g(\tilde{\mathbf{P}}_k, \mathbf{v}) = \exp \left(- \frac{|\mathbf{h}_k^H \tilde{\mathbf{P}}_k \mathbf{v}|^2}{\|\mathbf{h}_k^H \tilde{\mathbf{P}}_k \mathbf{I}_j\|^2 + 2\sigma_z^2} \right) \quad (12)$$

$$h(\tilde{\mathbf{P}}_k, \mathbf{w}) = \exp \left(- \frac{|\mathbf{h}_k^H \tilde{\mathbf{P}}_k \mathbf{w}|^2}{\|\mathbf{h}_k^H \tilde{\mathbf{P}}_k \mathbf{I}_j\|^2 + 2\sigma_z^2} \right) \quad (13)$$

$$g_1(\tilde{\mathbf{P}}_k, \mathbf{v}) = g(\tilde{\mathbf{P}}_k, \mathbf{v}) \left(\frac{- \left(\|\mathbf{h}_k^H \tilde{\mathbf{P}}_k \mathbf{I}_j\|^2 + 2\sigma_z^2 \right) \mathbf{h}_k \mathbf{h}_k^H \tilde{\mathbf{P}}_k \mathbf{v} \mathbf{v}^H + (\mathbf{v}^H \tilde{\mathbf{P}}_k^H \mathbf{h}_k \mathbf{h}_k^H \tilde{\mathbf{P}}_k \mathbf{v}) \mathbf{h}_k \mathbf{h}_k^H \tilde{\mathbf{P}}_k \mathbf{I}_j \mathbf{I}_j^H}{\left(\|\mathbf{h}_k^H \tilde{\mathbf{P}}_k \mathbf{I}_j\|^2 + 2\sigma_z^2 \right)^2} \right) \quad (14)$$

$$h_1(\tilde{\mathbf{P}}_k, \mathbf{w}) = h(\tilde{\mathbf{P}}_k, \mathbf{w}) \left(\frac{- \left(\|\mathbf{h}_k^H \tilde{\mathbf{P}}_k \mathbf{I}_j\|^2 + 2\sigma_z^2 \right) \mathbf{h}_k \mathbf{h}_k^H \tilde{\mathbf{P}}_k \mathbf{w} \mathbf{w}^H + (\mathbf{w}^H \tilde{\mathbf{P}}_k^H \mathbf{h}_k \mathbf{h}_k^H \tilde{\mathbf{P}}_k \mathbf{w}) \mathbf{h}_k \mathbf{h}_k^H \tilde{\mathbf{P}}_k \mathbf{I}_j \mathbf{I}_j^H}{\left(\|\mathbf{h}_k^H \tilde{\mathbf{P}}_k \mathbf{I}_j\|^2 + 2\sigma_z^2 \right)^2} \right) \quad (15)$$

interference signals increases. In this work, we are interested in a suboptimal (mismatched) decoding metric given by

$$q(x, y_k) = \sum_{\bar{\mathbf{i}} \in \mathcal{I}} \exp \left(- \frac{|y_k - \mathbf{h}_k^H \mathbf{P}_i \bar{\mathbf{i}} - \mathbf{h}_k^H \mathbf{p}_x x|^2}{\|\mathbf{h}_k^H \mathbf{P}_j\|^2 + \sigma_z^2} \right). \quad (8)$$

The philosophy of (8) is that the decoder uses full knowledge of \mathbf{i} and treats \mathbf{j} as Gaussian noise with the same variance. In fact, if $\mathbf{j} \sim \mathcal{CN}(\mathbf{0}^{\dim(\mathbf{j}) \times 1}, \mathbf{I}^{\dim(\mathbf{j})})$, (8) is the optimal decoding metric for (4). It can be observed that the computational complexity of (8) depends only on \mathbf{i} but not on \mathbf{j} , and is less than (7) by a factor of $|\mathcal{J}|$.

For mismatched decoding problems, the GMI gives the highest achievable rate under the i.i.d. random coding ensemble [19]. For the decoding metric given by (8), the GMI is given by (9) and is approximated by (10). To enable optimization of GMI, the gradient of GMI w.r.t. precoders is given by (11), where $g(\tilde{\mathbf{P}}_k, \mathbf{v})$, $h(\tilde{\mathbf{P}}_k, \mathbf{w})$, $g_1(\tilde{\mathbf{P}}_k, \mathbf{v})$ and $h_1(\tilde{\mathbf{P}}_k, \mathbf{w})$ are given by (12-15), with

$$\tilde{\mathbf{P}}_k = [\mathbf{p}_x \mathbf{P}_i \mathbf{P}_j], \quad (16)$$

$$\mathbf{v} = [x - \bar{x}; \mathbf{i} - \bar{\mathbf{i}}; \mathbf{j}], \quad (17)$$

$$\mathbf{w} = [\mathbf{0}^{\dim(\mathcal{X}) \times 1}; \mathbf{i} - \bar{\mathbf{i}}; \mathbf{j}], \quad (18)$$

$$\mathbf{I}_j = [\mathbf{0}^{\dim(\mathcal{X}) \times \dim(\mathcal{J})}; \mathbf{0}^{\dim(\mathcal{I}) \times \dim(\mathcal{J})}; \mathbf{I}^{\dim(\mathcal{J})}]. \quad (19)$$

Note that $\tilde{\mathbf{P}}_k$ is a column-wise permutation of the precoding matrix at the transmitter based on user- k 's decoding strategy.

B. Evaluation of RSMA and CS-RSMA

We assume that each user applies a suboptimal decoding strategy by treating the desired signals optimally but the undesired signals as Gaussian random variables with the same variance². For example, when user- k decodes s_c ,

²This decoding strategy is based on implications on soft codeword level interference cancellation for SIC receivers, and joint-demapping receivers for non-SIC receivers proposed in [5]. It assumes that the decoding metrics for common and private streams are separable. The joint-demapping receiver is classified as a non-SIC receiver in [5], which effectively treats the desired signals optimally when demodulating a stream. This is not the only possible decoding strategy. For clarity, we leave the analysis for other decoding strategies for future works.

it treats $\mathbf{h}_k^H \mathbf{p}_{k, s_{p,k}}$ optimally, but treats $\{\mathbf{h}_k^H \mathbf{p}_{k', s_{k'}}\}$ as $\mathcal{CN}(0, |\mathbf{h}_k^H \mathbf{p}_{k'}|^2)$, $\forall k' \in \mathcal{K}/k$. This decoding strategy is based on the assumption that desired signals are typically stronger than unwanted signals. An implication of [20] is that treating strong interference as Gaussian random variables can lead to significant losses, whereas the impact of treating weak interference as Gaussian random variables can be negligible. Hence, we consider decoders that treat the desired signals optimally to enable high performance under limited allowance for decoding complexity.

The instantaneous achievable information rates of the common and desired private streams at user- k can be measured by GMI as follows:

- For the common stream:

$$I_{c,k} = I_{\text{GMI}} \left(\mathbf{h}_k^H \mathbf{p}_c \mathcal{X}_c, \mathbf{h}_k^H \mathbf{p}_k \mathcal{X}_{p,k}, \sum_{k' \neq k} \mathbf{h}_k^H \mathbf{p}_{k'} \mathcal{X}_{p,k'}, \sigma_z^2 \right). \quad (20)$$

- For the private stream assuming SIC is applied to remove the common stream signal:

$$I_{p,k}^{\text{SIC}} = I_{\text{GMI}} \left(\mathbf{h}_k^H \mathbf{p}_k \mathcal{X}_{p,k}, \{0\}, \sum_{k' \neq k} \mathbf{h}_k^H \mathbf{p}_{k'} \mathcal{X}_{p,k'}, \sigma_z^2 \right). \quad (21)$$

- For the private stream assuming SIC-free receivers, i.e., the decoding of the private stream is under interference from the common stream:

$$I_{p,k}^{\text{non-SIC}} = I_{\text{GMI}} \left(\mathbf{h}_k^H \mathbf{p}_k \mathcal{X}_{p,k}, \mathbf{h}_k^H \mathbf{p}_c \mathcal{X}_c, \sum_{k' \neq k} \mathbf{h}_k^H \mathbf{p}_{k'} \mathcal{X}_{p,k'}, \sigma_z^2 \right). \quad (22)$$

$\forall k \in \mathcal{K}$, let c_k denote the portion of W_c occupied by $W_{c,k}$ in conventional RSMA, or the portion of s_c occupied by $s_{c,k}$ in CS-RSMA. Therefore, $c_k \geq 0$ and $\sum_{k \in \mathcal{K}} c_k = 1$.

Under different RSMA schemes, the achievable rate for user- k is expressed as follows:

- Conventional RSMA with SIC:

$$I_{\text{GMI},k} = c_k \min_{k' \in \mathcal{K}} I_{c,k'} + I_{p,k}^{\text{SIC}}. \quad (23)$$

- Conventional RSMA with SIC-free receivers:

$$I_{\text{GMI},k} = c_k \min_{k' \in \mathcal{K}} I_{c,k'} + I_{p,k}^{\text{non-SIC}}. \quad (24)$$

- CS-RSMA:

$$I_{\text{GMI},k} = c_k I_{c,k} + I_{p,k}^{\text{non-SIC}}. \quad (25)$$

Remark 1: The "min" operator in (23) and (24) is due to the fact that conventional RSMA requires all users to be able to decode the common stream. For CS-RSMA, users only need to decode the codeword after combining the segments from the common and private streams, and do not need to decode the common stream. The achievable rate at user- k is therefore given by a weighted average of the common stream rate and the private stream rate, with the weights determined by the ratio of symbols assigned to the two streams. Hence, the "min" operator disappears in (25).

Remark 2: The common stream in CS-RSMA is a combination of codeword segments from potentially all the users, and is not meant to be decodable to any of the users. Therefore, applying SIC to decode and remove the common stream is not feasible for CS-RSMA. Since the private stream is disrupted by interference from the common stream in decoding, in (25), the achievable rate contributed by the private stream is the same as in conventional SIC-free RSMA, assuming that the decoding metrics for the common and desired streams are separable.

C. Constrained Decoding Complexity

Comparing communication schemes in the finite alphabet regime is more involved than in the Gaussian signaling regime. On the one hand, the achievable rate ultimately depends on the cardinality of alphabets under sufficient SNR. On the other hand, the decoding complexity is proportional to the number of observed signals and the cardinality of their alphabets, which can be observed from (7) and (8). Therefore, we introduce the concept of decoding complexity constraint to ensure fairness of comparison.

Definition 1 (Decoding Complexity): A decoder of complexity- δ can compute " $\exp(|\cdot|^2)$ " for at most n times for each received symbol.

For example, for the channel model given by (4), the matched decoding, as in (7), is only valid if $\delta \geq |\mathcal{X}||\mathcal{I}||\mathcal{J}|$. The mismatched decoder given by (8) is valid if $\delta \geq |\mathcal{X}||\mathcal{I}|$, therefore, requires a lower decoding complexity than the matched decoding.

Proposition 1 (Decoding Complexity of RSMA): For conventional RSMA (with or without SIC) and CS-RSMA, if user- k treats all the undesired private streams as Gaussian noise, the decoding is feasible with at least complexity- $|\mathcal{X}_c||\mathcal{X}_{p,k}|$ at user- k , $\forall k \in \mathcal{K}$.

Proof: For all the RSMA schemes considered, we show that, if user- k treats all the undesired private streams as Gaussian random variables, it needs to compute

$$d(s_c, s_{p,k}, y_{t,k}) = \exp \left(- \frac{|y_{t,k} - \mathbf{h}_k^H \mathbf{p}_c s_c - \mathbf{h}_k^H \mathbf{p}_k s_{p,k}|^2}{\sum_{k' \neq k} |\mathbf{h}_k^H \mathbf{p}_{k'}|^2 + \sigma_z^2} \right) \quad (26)$$

$\forall s_c \in \mathcal{X}_c$, $\forall s_{p,k} \in \mathcal{X}_{p,k}$ and for each time instance t . The rest of the decoding is achieved by only summing and multiplying $d(s_c, s_{p,k}, y_{t,k})$ with different arguments. The exact decoders in terms of $d(s_c, s_{p,k}, y_{t,k})$ are listed as follows:

- For conventional RSMA, Let $\{s_c^{(1)}, \dots, s_c^{(M_c)}\}$ denote the codebook for common stream and $\{s_{p,k}^{(1)}, \dots, s_{p,k}^{(M_{p,k})}\}$ denote the codebook for the private stream intended for user- k , $\forall k \in \mathcal{K}$, with M_c and $M_{p,k}$ being the corresponding codebook sizes. Let $s_{c,t}^{(q)}$ and $s_{p,t,k}^{(q)}$ respectively denote the symbol of $s_c^{(q)}$ and $s_{p,k}^{(q)}$ at time instance t . The decoder for the common stream can be represented as

$$\begin{aligned} \widehat{W}_c &= \arg \max_{q \in 1, \dots, M_c} q^n(s_c^{(q)}, \mathbf{y}_k) \\ &= \arg \max_{q \in 1, \dots, M_c} \prod_{t=1}^n \sum_{s_{p,k} \in \mathcal{X}_{p,k}} d(s_{c,t}^{(q)}, s_{p,k}, y_{t,k}). \end{aligned} \quad (27)$$

If SIC is applied, the decoder for the private stream is based on \widehat{W}_c and can be represented as

$$\begin{aligned}\widehat{W}_k &= \arg \max_{q \in 1, \dots, M_{p,k}} q^n(\mathbf{s}_{p,k,t}^{(q)}, \mathbf{y}_k) \\ &= \arg \max_{q \in 1, \dots, M_{p,k}} \prod_{t=1}^n d(s_{c,t}^{(\widehat{W}_c)}, s_{p,t,k}^{(q)}, y_{t,k}).\end{aligned}\quad (28)$$

If SIC is not applied,

$$\begin{aligned}\widehat{W}_k &= \arg \max_{q \in 1, \dots, M_k} q^n(\mathbf{s}_{p,k}^{(q)}, \mathbf{y}_k) \\ &= \arg \max_{q \in 1, \dots, M_k} \prod_{t=1}^n \sum_{s_c \in \mathcal{X}_c} d(s_c, s_{p,t,k}^{(q)}, y_{t,k}).\end{aligned}\quad (29)$$

- For CS-RSMA, let $\{\mathbf{s}_k^{(1)}, \dots, \mathbf{s}_k^{(M_k)}\}$ represent the codebook for user- k with M_k being the codebook size, $\forall k \in \mathcal{K}$, and $s_{t,k}^{(q)}$ represent the symbol of q -th codeword at time instance t . The decoder can be represented as

$$\begin{aligned}\widehat{W}_k &= \arg \max_{q \in 1, \dots, M_k} q^n(\mathbf{s}_k^{(q)}, \mathbf{y}_k) \\ &= \arg \max_{q \in 1, \dots, M_k} \prod_{t' \in \mathcal{T}_k} \sum_{s_k \in \mathcal{X}_{p,k}} d(s_{\tau_c(t'),k}^{(q)}, s_k, y_{t,k}) \\ &\quad \prod_{t=1}^n \sum_{s_c \in \mathcal{X}_c} d(s_c, s_{\tau_{p,k}(t),k}^{(q)}, y_{t,k}),\end{aligned}\quad (30)$$

where \mathcal{T}_k represents the time indices where the symbols of s_c are generated from $s_{c,k}$, and $\tau_c(\cdot)$ and $\tau_{p,k}(\cdot)$ respectively maps the time index into the corresponding symbol index of user- k 's codeword.

Hence, computing $d(s_c, s_{p,k}, y_{t,k})$, $\forall s_c \in \mathcal{X}_c$ and $\forall s_{p,k} \in \mathcal{X}_{p,k}$, covers all "exp($|\cdot|^2$)" operations required for (27)-(29). This proves that complexity- δ is sufficient to decode conventional RSMA and CS-RSMA. It is also necessary to compute $d(s_c, s_{p,k}, y_{t,k})$, $\forall s_c \in \mathcal{X}_c$ and $\forall s_{p,k} \in \mathcal{X}_{p,k}$, as long as, at each time instance and for each stream, the probability of any symbol in the alphabet occurring is non-zero. ■

IV. PRECODER OPTIMIZATION

We propose precoder optimization algorithms for SR and MMF optimization under finite alphabets and suboptimal decoders. The alphabets are assumed to be fixed in this section, but will be allowed to adjust adaptively in Section V. To reduce computational complexity, the approximation given by (10) is utilized in the optimization, but the performance evaluation in Section V will be based on the exact GMI given by (9).

A. Sum-Rate Optimization

We consider a sum-rate maximization problem as follows:

$$\begin{aligned}\mathcal{P}_1: & \max_{\mathbf{P}, \mathbf{c}} \sum_{k \in \mathcal{K}} I_{\text{GMI},k} \\ \text{s.t. } & \|\mathbf{P}\|_{\text{F}}^2 \leq P_{\text{T}} \\ & \mathbf{c}^T \mathbf{1} = 1 \\ & \mathbf{c} \succcurlyeq \mathbf{0},\end{aligned}\quad (31)$$

where $\mathbf{c} = [c_1, c_2, \dots, c_K]^T$.

Proposition 2 (Sum-rate maximization reformulation): Under different RSMA schemes, \mathcal{P}_1 can be simplified into the following formulations:

- For conventional RSMA with or without SIC,

$$\begin{aligned}\mathcal{P}_2: & \max_{\mathbf{P}} \min_{k \in \mathcal{K}} I_{c,k} + \sum_{k \in \mathcal{K}} I_{p,k}^{\text{SIC/non-SIC}} \\ \text{s.t. } & \|\mathbf{P}\|_{\text{F}}^2 \leq P_{\text{T}}.\end{aligned}\quad (32)$$

- For CS-RSMA,

$$\begin{aligned}\mathcal{P}_3: & \max_{\mathbf{P}, \mathbf{c}} \max_{k \in \mathcal{K}} I_{c,k} + \sum_{k \in \mathcal{K}} I_{p,k}^{\text{non-SIC}} \\ \text{s.t. } & \|\mathbf{P}\|_{\text{F}}^2 \leq P_{\text{T}}.\end{aligned}\quad (33)$$

Proof: (32) is readily seen by substituting (23) and (24) into (31). For (33), substituting (25) into (31) leads to the following objective function:

$$\sum_{k \in \mathcal{K}} c_k I_{c,k} + \sum_{k \in \mathcal{K}} I_{p,k}^{\text{non-SIC}}. \quad (34)$$

It is trivial to see that the optimal \mathbf{c} is always given by having $c_k = 1$ for $k = \arg \max_k I_{c,k}$, and $c_{k'} = 0$ for $k' \neq k$. Using this optimal \mathbf{c} results in (33). ■

Remark 3: An interesting difference between \mathcal{P}_2 and \mathcal{P}_3 is that the "min" operator in \mathcal{P}_2 is replaced by "max" in \mathcal{P}_3 . This indicates that CS-RSMA is expected to perform at least as well as conventional RSMA without SIC in SR, since its problem formulation only differs from the latter by changing the "min" to a "max". The ranking between CS-RSMA and conventional RSMA with SIC is difficult to reveal analytically because, although CS-RSMA is disadvantaged in the omission of SIC, its common stream is not restricted to be decodable by all the users.

Remark 4: To achieve the maximum SR of CS-RSMA, if the common stream is activated, the number of codewords to split is strictly one. In contrast, in conventional RSMA, the number of messages to split can be any number between 1 and K , as discussed in [7].

We further reformulate the problems in Proposition 2 using the logarithmic barrier [21] to approximate \mathcal{P}_2 and \mathcal{P}_3 as the following unconstrained optimization problem:

$$\mathcal{P}_4: \max_{\mathbf{P}, \mathbf{c}} \tau I_{\text{sum}} + \log(P_{\text{T}} - \|\mathbf{P}\|_{\text{F}}^2), \quad (35)$$

where I_{sum} represents the objective function of \mathcal{P}_2 and \mathcal{P}_3 depending on the RSMA scheme in use, and τ is a parameter that sets the accuracy of the approximation.

For RSMA with SIC, one subgradient of I_{sum} w.r.t. \mathbf{P} is given by

$$g(I_{\text{sum}}) = \nabla_{\mathbf{P}} I_{c,k'} + \sum_{k \in \mathcal{K}} \nabla_{\mathbf{P}} I_{p,k}^{\text{SIC}}, \quad (36)$$

where $k' = \arg \min_k I_{c,k}$. For RSMA without SIC and CS-RSMA,

$$g(I_{\text{sum}}) = \nabla_{\mathbf{P}} I_{c,k'} + \sum_{k \in \mathcal{K}} \nabla_{\mathbf{P}} I_{p,k}^{\text{non-SIC}}, \quad (37)$$

where, for RSMA without SIC, $k' = \arg \min_k I_{c,k}$ and, for CS-RSMA, $k' = \arg \max_k I_{c,k}$. The gradients in (36) and (37) can be computed by referring to (20)-(22) and (11).

Algorithm 1 Subgradient Ascent with Barrier Method for Sum-Rate Maximization

Input: $P_T, \mathcal{K}_c, \mathcal{K}_{p,k}, \mathbf{h}_k, k \in \mathcal{K}, \beta, \epsilon, v_{\max}, \tau_{\max}$.

Output: \mathbf{P}^*

```

1: Initialize  $\mathbf{P}^0$  and  $\tau$ .
2: repeat
3:    $v := 0$ .
4:   repeat
5:      $\Delta \mathbf{P} := \tau g(I_{\text{sum}}) + \frac{\mathbf{P}^v}{\|\mathbf{P}^v\|_F^2 - P_T}$ .
6:     Choose step size  $\alpha$  via backtracking line search.
7:     Update.  $\mathbf{P}^{v+1} := \mathbf{P}^v + \alpha \Delta \mathbf{P}$ .
8:     Update.  $\Omega_{\text{SR}}^{v+1} := \Omega_{\text{SR}}(\mathbf{P}^{v+1})$ .
9:      $v := v + 1$ .
10:  until  $|\Omega_{\text{SR}}^v - \Omega_{\text{SR}}^{v-1}| < \epsilon$  or  $v \geq v_{\max}$ .
11:  Update  $\tau := \beta \tau$ .
12: until  $\tau \geq \tau_{\max}$ .
13: return  $\mathbf{P}^* := \mathbf{P}^v$ .
```

It can be noticed that the problems described by $\mathcal{P}_1 - \mathcal{P}_4$ are non-convex due to the non-convexity of (9) and (10) w.r.t. the precoders, and non-smooth due to the "min/max" operators over k . Hence, it is difficult to obtain the global optimal solutions of them. We use the subgradient descent method to optimize \mathcal{P}_4 . The complete algorithm is summarized in Alg. 1, with $\Omega_{\text{SR}}(\mathbf{P})$ representing the objective function in \mathcal{P}_4 . Alg. 1 is guaranteed to converge because each update on \mathbf{P} leads to a non-decreasing update on the objective function, and the objective function is clearly upper-bounded.

B. Minimum Rate Optimization

We now consider a max-min fairness problem as follows:

$$\begin{aligned}
\mathcal{P}_5: \max_{\mathbf{P}, \mathbf{c}} \min_{k \in \mathcal{K}} I_{\text{GMI},k} \\
\text{s.t. } \|\mathbf{P}\|_F^2 \leq P_T \\
\mathbf{c}^T \mathbf{1} = 1 \\
\mathbf{c} \succeq \mathbf{0}.
\end{aligned} \tag{38}$$

\mathcal{P}_5 is a non-convex problem. To solve it efficiently, we decouple it into the following two sub-problems,

$$\begin{aligned}
\mathcal{P}_6: \max_{\mathbf{c}} \min_{k \in \mathcal{K}} I_{\text{GMI},k}(\mathbf{c}; \mathbf{P}) \\
\text{s.t. } \mathbf{c}^T \mathbf{1} = 1 \\
\mathbf{c} \succeq \mathbf{0},
\end{aligned} \tag{39}$$

and

$$\begin{aligned}
\mathcal{P}_7: \max_{\mathbf{P}} \min_{k \in \mathcal{K}} I_{\text{GMI},k}(\mathbf{P}; \mathbf{c}) \\
\text{s.t. } \|\mathbf{P}\|_F^2 \leq P_T.
\end{aligned} \tag{40}$$

\mathcal{P}_6 optimizes \mathbf{c} with a fixed \mathbf{P} , whereas \mathcal{P}_7 optimizes \mathbf{P} with a given \mathbf{c} . Note that \mathcal{P}_6 is a linear programming, and hence its global optimal solution can be efficiently obtained. In particular, we developed a closed-form solution as in Proposition 3.

Proposition 3: The global optimal solution of \mathcal{P}_6 is given in closed form by Alg. 2.

Proof: See Appendix B. ■

Algorithm 2 Global Optimal Common Stream Allocation

Input: $I_{c,k}, I_{p,k}, k \in \mathcal{K}$.

Output: \mathbf{c}^*

```

1:  $I'_{c,k} := \min_k I_{c,k}$  for conventional RSMA and
    $I'_{c,k} := I_{c,k}$  for CS-RSMA.
2:  $k' := K$ .
3: repeat
4:    $\mathbf{A} := \text{diag}\{[I'_{c,1}, \dots, I'_{c,k'}]\}$ ,  $\mathbf{b} := [I_{p,1}, \dots, I_{p,k'}]^T$ .
5:    $\xi := \frac{1 + \mathbf{1}^T \mathbf{A}^{-1} \mathbf{b}}{\mathbf{1}^T \mathbf{A}^{-1} \mathbf{1}}$ .
6:    $\mathbf{c}' := \xi \mathbf{A}^{-1} \mathbf{1} - \mathbf{A}^{-1} \mathbf{b}$ .
7:    $k' := k' - 1$ .
8: until  $\mathbf{c}' \succeq \mathbf{0}$ .
9: return  $\mathbf{c}^* := [\mathbf{c}'^T, \mathbf{0}^{1 \times (K - k' - 1)}]^T$ .
```

To remove the discontinuity caused by the point-wise minimum in \mathcal{P}_7 , we apply a log-sum-exp approximation to its objective function and consider \mathcal{P}_8 as follows:

$$\begin{aligned}
\mathcal{P}_8: \max_{\mathbf{P}} \frac{1}{\gamma} \log \sum_{k \in \mathcal{K}} \exp(\beta I_{\text{GMI},k}(\mathbf{P}; \mathbf{c})) \\
\text{s.t. } \|\mathbf{P}\|_F^2 \leq P_T.
\end{aligned} \tag{41}$$

The gap between point-wise minimum and its log-sum-exp approximation is characterized by the following inequality [22],

$$0 \leq \min_{1 \leq i \leq L} f_i - \frac{1}{\gamma} \log \sum_{i=1}^L \exp(\gamma f_i) \leq \frac{1}{\gamma} \log L, \gamma < 0. \tag{42}$$

A subgradient of the objective function in \mathcal{P}_8 w.r.t. \mathbf{P} is derived to be

$$g(I_{\text{max-min}}) = \frac{1}{\gamma} \frac{\sum_{k \in \mathcal{K}} \beta \exp(\beta I_{\text{GMI},k}(\mathbf{P}; \mathbf{c})) g(I_{\text{GMI},k}(\mathbf{P}; \mathbf{c}))}{\sum_{k \in \mathcal{K}} \exp(\beta I_{\text{GMI},k}(\mathbf{P}; \mathbf{c}))}, \tag{43}$$

with

$$g(I_{\text{GMI},k}(\mathbf{P}; \mathbf{c})) = c_k g(I_c) + \nabla_{\mathbf{P}} I_{p,k}, \tag{44}$$

where $g(I_c) = \nabla_{\mathbf{P}} I_{c,k'}^{\text{SIC/non-SIC}}$ with $k' = \arg \min_k I_{c,k'}^{\text{SIC/non-SIC}}$ for RSMA with/without SIC, and $g(I_c) = \nabla_{\mathbf{P}} I_{c,k}^{\text{non-SIC}}$ for CS-RSMA.

Similarly to (35), the inequality constraint in \mathcal{P}_8 can be integrated into the objective function through the logarithmic barrier. This leads to

$$\mathcal{P}_9: \max_{\mathbf{P}} \frac{\tau}{\gamma} \log \sum_{k \in \mathcal{K}} \exp(\gamma I_{\text{GMI},k}(\mathbf{c})) + \log(P_T - \|\mathbf{P}\|_F^2). \tag{45}$$

\mathcal{P}_9 can be solved using subgradient ascent. The solution of \mathcal{P}_5 is obtained by solving \mathcal{P}_6 and \mathcal{P}_9 alternatively and the steps are summarized in Alg. 3, with $\Omega_{\text{MMF}}(\mathbf{P})$ representing the objective function in \mathcal{P}_9 . Alg. 3 is guaranteed to converge because each update on \mathbf{P} and \mathbf{c} leads to a non-decreasing update on the objective function, and the objective function is clearly upper-bounded.

V. NUMERICAL RESULTS ON PRECODER OPTIMIZATION FOR RSMA

In this section, we investigate the theoretical performance of CS-RSMA and conventional RSMA schemes under

Algorithm 3 Subgradient Ascent with Barrier Method for Max-Min Fairness

Input: $P_T, \mathcal{X}_c, \mathcal{X}_{p,k}, \mathbf{h}_k, k \in \mathcal{K}, \beta, \gamma, \epsilon, v_{\max}, \tau_{\max}$.

Output: \mathbf{P}^* and \mathbf{c}^*

- 1: Initialize \mathbf{P}^0 and τ .
 - 2: **repeat**
 - 3: $v := 0$.
 - 4: **repeat**
 - 5: Update $I_{c,k}, I_{p,k}$ based on \mathbf{P}^v .
 - 6: Update \mathbf{c} using Alg. 2.
 - 7: $\Delta \mathbf{P} := \tau g(I_{\max-\min}) + \frac{\mathbf{P}^v}{\|\mathbf{P}^v\|_F^2 - P_T}$.
 - 8: Choose step size α via backtracking line search.
 - 9: Update. $\mathbf{P}^{v+1} := \mathbf{P}^v + \alpha \Delta \mathbf{P}$.
 - 10: Update. $\Omega_{\text{MMF}}^{v+1} := \Omega_{\text{MMF}}(\mathbf{P}^{v+1})$.
 - 11: $v := v + 1$.
 - 12: **until** $|\Omega_{\text{MMF}}^v - \Omega_{\text{MMF}}^{v-1}| < \epsilon$ or $v \geq v_{\max}$.
 - 13: Update $\tau := \beta \tau$.
 - 14: **until** $\tau \geq \tau_{\max}$.
 - 15: **return** $\mathbf{P}^* := \mathbf{P}^v$ and $\mathbf{c}^* := \mathbf{c}$.
-

mismatched decoding through numerical simulations. Prior to the results, adaptive modulation and channel model will be introduced.

All the results in this section are ergodic performance measured by averaging 100 channel realizations. The precoder initialization in Alg. 1 and 3 involves the low-complexity precoders proposed in [5] for constellation-constrained sum-rate optimization and some randomly generated precoders.

A. Adaptive modulation

We assume that all the users are subject to a decoding complexity $\delta=4$ or 16^3 . The alphabets applied to the streams are chosen from BPSK and QAM constellations subject to the decoding complexity constraints. This leads to a few transmission modes in terms of alphabets for each complexity constraint, as summarized in Tables I and II. The simulations allow adaptive alphabet selection under certain decoding complexity.

Remark 5: With Mode 1 in both Tables I and II, RSMA becomes SDMA; with Mode 3 in Table I and Mode 5 in Table II, RSMA is equivalent to multicasting all messages [23].

Remark 6: Achievable rates under finite alphabets are upper-limited by the cardinality of the alphabets. Different transmission modes lead to different maximum achievable rates. It can be observed from Tables I and II that the sum rate of Mode 1, i.e., SDMA, is upper-bounded by $K \log_2 \delta$ bits and is the highest among all the modes, whereas the sum rate of multicasting, i.e., the last mode in both tables, is upper-bounded by $\log_2 \delta$ bits and is the lowest among all the modes. For example, for $K=2$ and $\delta=16$, Mode 1 can bring at most 8 bits per transmission in SR, which cannot be achieved by any other mode.

³It is assumed that δ is the same for all the users for simplicity and clarity. The problem and solution introduced in Section IV can be trivially generalized to ones with non-uniform complexity constraints among users.

TABLE I
TRANSMISSION MODES UNDER DECODING COMPLEXITY $\delta=4$

Mode	1	2	3
Private Stream	QPSK	BPSK	{0}
Common Stream	{0}	BPSK	QPSK

TABLE II
TRANSMISSION MODES UNDER DECODING COMPLEXITY $\delta=16$

Mode	1	2	3	4	5
Private Stream	16QAM	8QAM	QPSK	BPSK	{0}
Common Stream	{0}	BPSK	QPSK	8QAM	16QAM

B. Channel model

The spatially correlated Rayleigh-fading channel is given by $\mathbf{h}_k \sim \mathcal{CN}(\mathbf{0}^{N_T \times 1}, \mathbf{R}_k)$, where $\mathbf{R}_k \in \mathbb{C}^{N_T \times N_T}$ is the channel covariance matrix for user- k . With eigendecomposition to \mathbf{R}_k ,

$$\mathbf{R}_k = \mathbf{U}_k \mathbf{\Lambda}_k \mathbf{U}_k^H, \quad (46)$$

where $\mathbf{\Lambda}_k$ is a $r_k \times r_k$ diagonal matrix containing the nonzero eigenvalues of \mathbf{R}_k and $\mathbf{U}_k \in \mathbb{C}^{N_T \times r_k}$ contains the eigenvectors of \mathbf{R}_k corresponding to the nonzero eigenvalues. The Karhunen-Loeve representation of \mathbf{h}_k gives

$$\mathbf{h}_k = \mathbf{U}_k \mathbf{\Lambda}_k^{\frac{1}{2}} \mathbf{w}_k, \quad (47)$$

where $\mathbf{w}_k \in \mathbb{C}^{r_k \times 1} \sim \mathcal{CN}(\mathbf{0}^{r_k \times 1}, \mathbf{I}^{r_k})$.

We follow the one-ring scattering model proposed in [24], which assumes that there is no line-of-sight path between the transmitter and user- k and the angle-of-departure of all scatters is uniformly distributed around a centre angle-of-departure, θ_k , with an angular spread of Δ_k for user- k . Consider a uniform and linear antenna array with the spacing between the antenna elements to be $\lambda/2$, where λ denotes the wavelength, elements of \mathbf{R}_k are given by

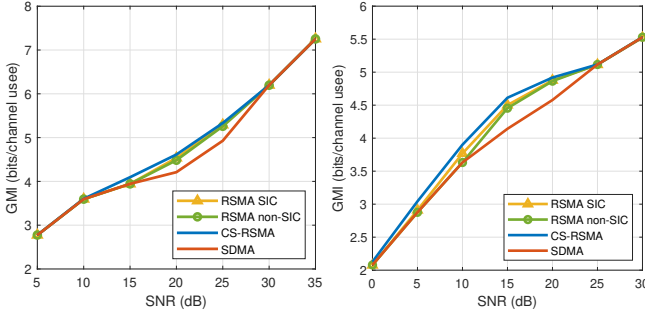
$$[\mathbf{R}_k]_{m,n} = \frac{1}{2\Delta_k} \int_{-\Delta_k}^{\Delta_k} e^{-j\pi(\alpha+\theta_k)(m-n)\sin\alpha} d\alpha. \quad (48)$$

We assume that $\theta_k = \pi/3$ and $\Delta_k = \Delta, \forall k \in \mathcal{K}$, which implies that users with similar channel statistics are served at the same time. The purpose of this setting is to model communication scenarios with a certain user density.

C. Sum-rate evaluation

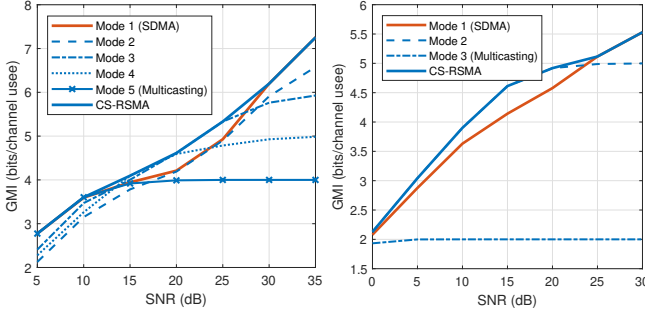
Fig. 3 depicts the ergodic SR performance of conventional RSMA schemes, CS-RSMA and SDMA. It can be observed that RSMA schemes, including CS-RSMA, bring benefits in the medium SNR regime compared to SDMA. Furthermore, CS-RSMA slightly outperforms conventional RSMA schemes. The ergodic SR led by different transmission modes under CS-RSMA is depicted in Fig. 4, together with the performance of CS-RSMA given by adaptive alphabet/mode selection as a reference. It can be observed that the transmission modes that enable the common stream achieve higher SR than Mode 1, i.e., SDMA, at medium SNR. At high SNR, Mode 1 dominates as other modes saturate at lower SR, as suggested by Remark 6.

Fig. 5 depicts the ergodic rates of common and private streams under CS-RSMA and conventional RSMA. It can



(a) $N_T = 2, K = 2, \Delta = \pi/18, \delta = 16$. (b) $N_T = 4, K = 4, \Delta = \pi/12, \delta = 4$.

Fig. 3. Ergodic SR performance of conventional RSMA, CS-RSMA and SDMA.



(a) $N_T = 2, K = 2, \Delta = \pi/18, \delta = 16$. (b) $N_T = 4, K = 4, \Delta = \pi/12, \delta = 4$.

Fig. 4. Ergodic SR performance of different modes of CS-RSMA.

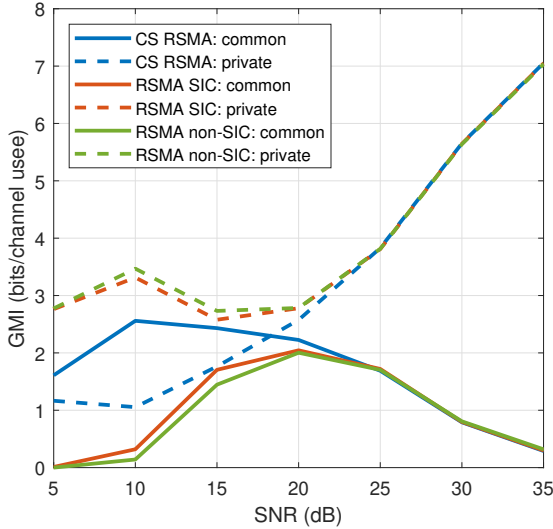
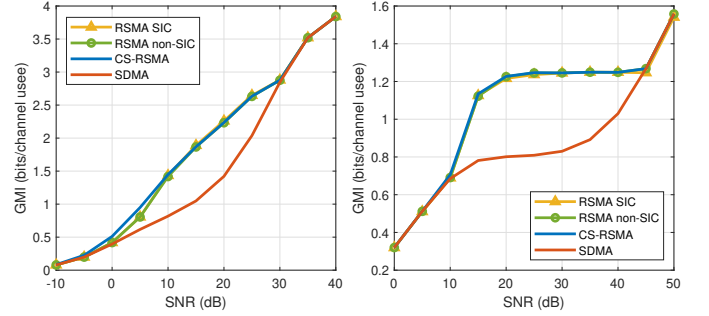


Fig. 5. Comparing common and private stream rates with $N_T = 2, K = 2, \Delta = \pi/18, \delta = 16$.

be observed that CS-RSMA tends to carry more information rates in the common stream than conventional RSMA. This is a consequence of having "max" on the common rates in the SR problem formulation for CS-RSMA instead of the "min" in the one for conventional RSMA, as shown in \mathcal{P}_2 and \mathcal{P}_3 .

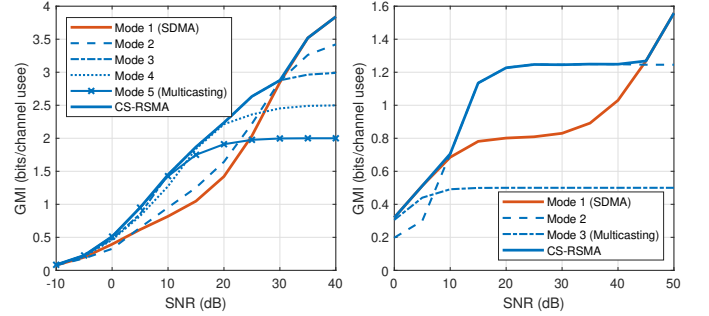
D. Max-min fairness optimization

Fig. 6 depicts the ergodic MMF performance of conventional RSMA schemes, CS-RSMA and SDMA. Similarly to



(a) $N_T = 2, K = 2, \Delta = \pi/18, \delta = 16$. (b) $N_T = 4, K = 4, \Delta = \pi/9, \delta = 4$.

Fig. 6. Ergodic MMF performance of conventional RSMA, CS-RSMA and SDMA.



(a) $N_T = 2, K = 2, \Delta = \pi/18, \delta = 16$. (b) $N_T = 4, K = 4, \Delta = \pi/9, \delta = 4$.

Fig. 7. Ergodic MMF performance of different modes of CS-RSMA.

SR performance, RSMA brings benefits at the medium SNR regime by activating the common stream, but converges to SDMA at high SNR regime. CS-RSMA performs very similar to conventional RSMA schemes⁴. The performance of different modes of CS-RSMA is depicted in Fig. 7, along with the performance of CS-RSMA given by adaptive alphabet/mode selection as a reference. It shows that activating the common stream brings higher minimum rates among users under medium SNR than Mode 1, i.e., SDMA, whereas Mode 1 dominates under high SNR, because the modes enabling the common stream saturates at lower rates, as suggested by Remark 6.

VI. PHY TRANSCEIVER DESIGN FOR CS-RSMA AND LINK-LEVEL SIMULATION

In this section, we propose a transceiver architecture for CS-RSMA and evaluate its performance using link-level simulations.

A. PHY Transceiver Design

Fig. 8 depicts the proposed CS-RSMA transmitter architecture, where "FEC" and "Mod" represent forward error

⁴For both SR and MMF evaluation, if the input signals are not from finite alphabets but are Gaussian distributed, the gap between RSMA with SIC and SDMA exists in both medium and high SNR regime, as shown in [11], [25], because the common stream rate will not saturate at high SNR. CS-RSMA, SIC-free RSMA and SDMA will perform similarly under Gaussian input, because the interference from the common stream when decoding the private stream is more detrimental than with finite-alphabet inputs.

correction coding⁵ and modulation (mapping) respectively. For clarity, the time index is neglected in the notation. In Fig. 8, the messages, W_1, W_2, \dots, W_K , are first encoded into binary codewords, denoted by X_1, X_2, \dots, X_K . Codeword segmentation and combining can be achieved by de-multiplexing and multiplexing the encoded bits into $X_c, X_{p,1}, X_{p,2}, \dots, X_{p,K}$. The common and private streams are obtained by modulating the resulting $K + 1$ bit streams into symbol streams. The precoders then mix the symbol streams into a stream of vector symbols to feed the multiple transmit antennas. The resource mapper allocates different instances of the vector symbol stream to different physical layer resource elements⁶.

Fig. 9 depicts two proposed receiver architectures for CS-RSMA, where "FEC⁻¹" and "Demod" represent channel decoder and demodulator (demapper) respectively. They are based on the joint de-mapping receiver and soft Symbol Level Interference Cancellation (SLIC) receiver for conventional RSMA proposed in [5]. The two receiver architectures are explained as follows.

- 1) Joint de-mapping: The receiver first jointly demodulates the common stream and the desired private stream from the receiver signal. Assuming a soft-output demodulator is in use, the demodulator produces Log-Likelihood Ratios (LLRs) for X_c and $X_{p,k}$, denoted as LLR_c and $LLR_{p,k}$. The receiver then de-multiplexes (extracts) the LLRs for $X_{c,k}$ from LLR_c , denoted as $LLR_{c,k}$. $LLR_{c,k}$ and $LLR_{p,k}$ are then multiplexed (combined) into LLRs of the desired unicast message, X_k , denoted as LLR_k . Finally, the receiver decodes LLR_k into an estimate of the desired message \hat{W}_k .
- 2) Soft SLIC: Jointly demodulating X_c and $X_{p,k}$ may introduce a high computational burden, therefore, soft SLIC is proposed as a low-complexity alternative of joint demapping. With soft SLIC, the receiver first demodulates s_c by treating all private streams as Gaussian noise and obtains LLR_c . Based on LLR_c , the receiver then computes the posterior probability distribution of the common stream symbols, denoted by $P(s_c|y)$. $P(s_c|y)$ is used to compute the soft symbol estimates, i.e., $\mathbb{E}[s_c|y]$, denoted by \tilde{s} , and the variance of the residue noise, $\mathbb{E}[|s_c - \tilde{s}|^2|y]$, denoted as $\sigma_{s_c}^2$. Next, the receiver applies soft cancellation of s_c by subtracting $\mathbf{h}_k^H \mathbf{p}_c \tilde{s}$ from y_k and demodulates $s_{p,k}$ from the remaining signal into $LLR_{p,k}$. The remaining steps are the same as in the joint de-mapping implementation: the receiver de-multiplexes (extracts) $LLR_{c,k}$ from LLR_c , multiplexes $LLR_{c,k}$ and $LLR_{p,k}$ into LLR_k , and decodes \hat{W}_k based on LLR_k .

B. Link-Level Simulation

Link-level simulations were performed to evaluate the proposed CS-RSMA transceiver designs. In the following, we assume fast fading channels, where individual channel observations are generated using the one-ring channel model

⁵This potentially includes interleaving and scrambling.

⁶These can be created, for example, by Orthogonal Frequency-Division Multiplexing (OFDM) and Time Domain Multiplexing (TDM).

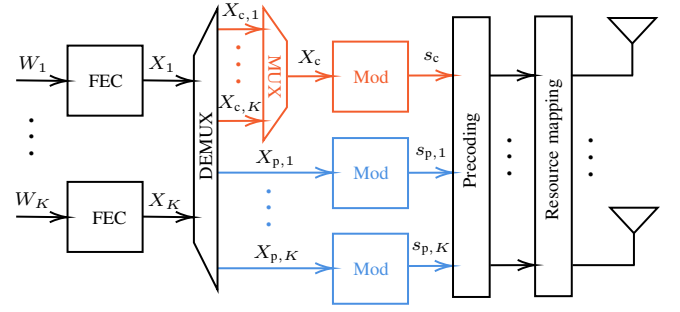


Fig. 8. PHY transmitter design for CS-RSMA.

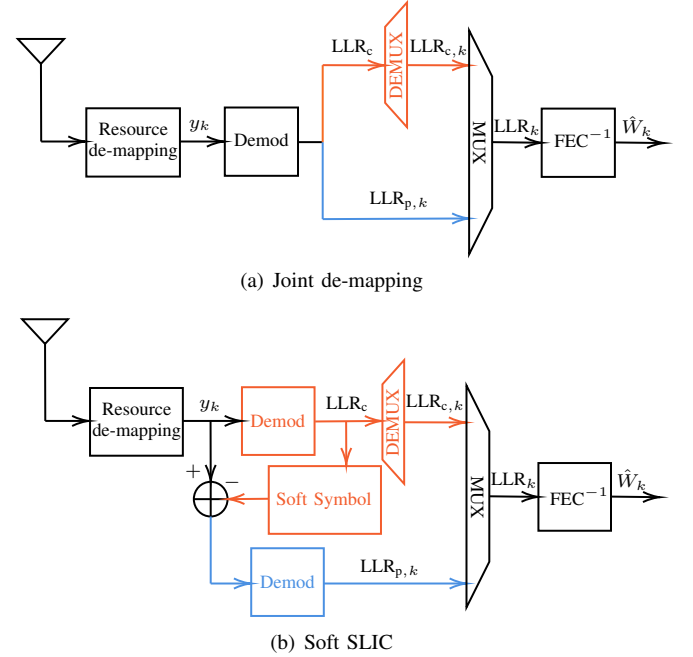


Fig. 9. PHY receiver designs for CS-RSMA.

introduced in Section V, with $N_T = 4$, $K = 2$, and $\Delta = \pi/18$. For channel encoding and decoding, LDPC code specified in 5G NR [26] with belief propagation decoding is chosen for its popularity and efficiency for long code lengths. All the BER results were obtained by averaging the results from 50000 blocks. The symbol block length is set to 512. For de-mapping, max-log approximation was applied for its popularity in practice. To reduce simulation time, the low-complexity precoder design proposed in [5] for RSMA without SIC is used for CS-RSMA.

Fig. 10 depicts BER curves of conventional RSMA and CS-RSMA with both joint de-mapping and soft SLIC receivers. It can be observed that, with the same receiver implementation, CS-RSMA performs slightly better than conventional RSMA. Taking 10^{-4} as the target BER, the SNR gap is around 0.05dB. The minor performance gap between CS-RSMA and conventional RSMA is consistent with the results from Section V. In addition, a soft SLIC receiver only leads to a minor performance loss compared to joint mapping, which is consistent with the observation in [5].

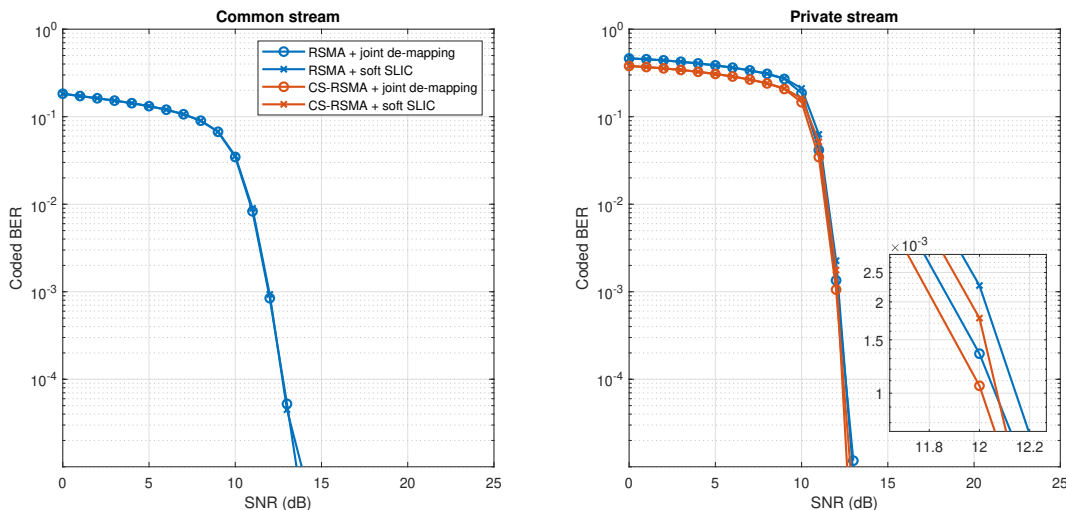


Fig. 10. BER comparison between conventional RSMA and CS-RSMA with all streams using QPSK constellation. Code rate for RSMA: 0.85 for common streams, 0.325 for private streams. Code rate for CS-RSMA: 0.5 for both streams.

C. Advantages of CS-RSMA

Although the numerical results in Section V and this section show that the achievable rate and BER performance of CS-RSMA is not significantly different from conventional RSMA, the introduction of CS-RSMA is of significant importance for practical applications. We briefly discuss these benefits of implementing CS-RSMA compared to conventional RSMA in the following aspects.

- 1) Reduced encoding/decoding complexity: With CS-RSMA, the transmitter encodes K messages rather than $K+1$ messages as in conventional RSMA; the receiver decodes one codeword rather than two as in conventional RSMA. The reduced number of codewords for each user leads not only to reduced encoding/decoding complexity but also simplification on error detection (e.g., CRC check), interleaving, and scrambling.
- 2) Reduced signaling overhead: With CS-RSMA, each receiver only needs information on the encoding scheme for one codeword, rather than two (for common and private streams) as with conventional RSMA. This leads to less requirements on control signaling from CS-RSMA.
- 3) Simplified retransmission design: With conventional RSMA, additional retransmission, e.g., Hybrid Automatic Repeat Request (HARQ), process needs to be implemented for the common stream. Due to the fact that the common stream is encoded with messages for potentially multiple users, designing the retransmission scheme for the common stream can be a complicated problem (some examples are given in [10]). With CS-RSMA, the retransmission mechanism only needs to be implemented for the K encoded unicast messages, exactly the same as the widely used MU-MIMO. This means that the existence of CS-RSMA can be transparent to the retransmission process for conventional MU-MIMO. For example, to implement RSMA in 5G NR PDSCH channels, CS-RSMA is naturally compatible with the existing

HARQ process, whereas conventional RSMA requires redesigning the HARQ process for the common stream.

Although this work only presents 1-layer CS-RSMA, i.e., with one common stream, the idea of codeword segmentation and creating common streams using part of segments can be trivially extended to multi-layer RSMA schemes, such as the hierarchical RSMA in [8] and the general framework of multi-layer RSMA in [9], where more common streams need to be implemented. In these cases, the above three benefits will be significantly magnified as the number of common streams increases.

Overall, CS-RSMA brings significant convenience in terms of complexity in implementation and compatibility with existing systems and performs slightly better than conventional RSMA without SIC.

VII. CONCLUSION

We proposed a novel architecture for RSMA, namely CS-RSMA. To capture practical constraints on receiver complexity, we evaluated the performance of conventional RSMA and CS-RSMA using the GMI for FAGCI channels, which assumes that users implement suboptimal decoders that treat undesired signals as Gaussian random variables for lower complexity. We further formulated SR and MMF optimization problems and developed optimization algorithms for precoder design. Numerical results on SR and MMF evaluations reveal that CS-RSMA slightly outperforms conventional RSMA schemes in SR, while performs very similar to them in MMF. Furthermore, PHY transceiver designs were proposed for CS-RSMA, and LLS were utilized to further evaluate CS-RSMA under the proposed transceiver implementations. Overall, we concluded that CS-RSMA performs very similar to conventional RSMA, and occasionally outperforms it, both under information-theoretical metrics and LLS. Last but not least, we discussed the significant practical benefits from CS-RSMA on encoding/decoding complexity, control signalling overhead, and retransmission mechanism design in comparison to the conventional RSMA.

APPENDIX A PROOF OF PROPOSITION 3

\mathcal{P}_7 can be written as follows:

$$\begin{aligned} \mathcal{P}_{10}: & \max_{\mathbf{c}} \min_k c_i I'_{c,k} + I_{p,k} \\ \text{s.t. } & \mathbf{c} \succcurlyeq \mathbf{0}, \\ & \mathbf{1}^T \mathbf{c} = 1. \end{aligned} \quad (49)$$

For conventional RSMA (either with or without SIC), $I'_{c,k} = \min_k I_{c,k}$, $\forall k \in \mathcal{K}$. For CS-RSMA, $I'_{c,k} = I_{c,k}$, $\forall k \in \mathcal{K}$.

By introducing a slack variable, ξ , \mathcal{P}_{10} can be converted into

$$\begin{aligned} \mathcal{P}_{11}: & \max_{\mathbf{c}} \xi \\ \text{s.t. } & \mathbf{c} \succcurlyeq \mathbf{0}, \\ & \mathbf{1}^T \mathbf{c} = 1. \\ & c_i I'_{c,k} + I_{p,k} \geq \xi, \forall k. \end{aligned} \quad (50)$$

WLOG, we assume $I_{p,1} < I_{p,2} < \dots < I_{p,K}$. Assume that the solution of \mathcal{P}_{11} leads to $c_i > 0$ for $k = 1, \dots, k'$. It is easy to see that $c_i I'_{c,k} + I_{p,k} = \xi$ for $k = 1, \dots, k'$. Equivalently,

$$\mathbf{A}\mathbf{c}' + \mathbf{b} = \xi \mathbf{1}, \quad (51)$$

where $\mathbf{A} = \text{diag}\{[I'_{c,1}, \dots, I'_{c,k'}]\}$, $\mathbf{b} = [I_{p,1}, \dots, I_{p,k'}]^T$, $\mathbf{c}' = [c_1, \dots, c_{k'}]^T$, and $\mathbf{1}$ is a column vector of length k' whose elements are all ones. The global optimal solution of \mathbf{c}' and ξ , ξ^* and \mathbf{c}'^* , can then be obtained by

$$\mathbf{c}'^* = \xi^* \mathbf{A}^{-1} \mathbf{1} - \mathbf{A}^{-1} \mathbf{b} \quad (52)$$

and

$$\xi^* = \frac{1 + \mathbf{1}^T \mathbf{A}^{-1} \mathbf{b}}{\mathbf{1}^T \mathbf{A}^{-1} \mathbf{1}}. \quad (53)$$

Note that (52) is directly from (51), and (53) is from (52) combined the condition of $\mathbf{1}^T \mathbf{c} = 1$.

Although k' , i.e., the number of users who are strictly served by the common stream, is still unknown, we can test it using (52) and (53). This is because allocating the common stream resource to more users than k' will lead to \mathbf{c}' containing negative entries, which is infeasible. Hence, by iteratively guessing the number of users to be served by the common stream, Alg. 2 is obtained.

REFERENCES

- [1] B. Clerckx, Y. Mao, Z. Yang, M. Chen, A. Alkhateeb, L. Liu, M. Qiu, J. Yuan, V. W. S. Wong, and J. Montojo, "Multiple access techniques for intelligent and multifunctional 6g: Tutorial, survey, and outlook," *Proceedings of the IEEE*, vol. 112, no. 7, pp. 832–879, 2024.
- [2] E. A. Jorswieck, "Next-generation multiple access: From basic principles to modern architectures," *Proceedings of the IEEE*, vol. 112, no. 9, pp. 1149–1178, 2024.
- [3] B. Clerckx, Y. Mao, E. A. Jorswieck, J. Yuan, D. J. Love, E. Erkip, and D. Niyato, "A primer on rate-splitting multiple access: Tutorial, myths, and frequently asked questions," *IEEE Journal on Selected Areas in Communications*, vol. 41, no. 5, pp. 1265–1308, 2023.
- [4] X. Lyu, S. Aditya, A. Kim, and B. Clerckx, "Rate-splitting multiple access: The first prototype and experimental validation of its superiority over SDMA and NOMA," *IEEE Transactions on Wireless Communications*, vol. 23, no. 8, pp. 9986–10000, 2024.
- [5] S. Zhang, B. Clerckx, D. Vargas, O. Haffenden, and A. Murphy, "Rate-splitting multiple access: Finite constellations, receiver design, and SIC-free implementation," *IEEE Transactions on Communications*, vol. 72, no. 9, pp. 5319–5333, 2024.
- [6] S. Zhang, B. Clerckx, and D. Vargas, "SIC-free rate-splitting multiple access: Constellation constrained sum-rate optimization," in *Proc. IEEE 25th Int. Workshop Signal Process. Adv. Wireless Commun. (SPAWC)*, Sep. 2024, pp. 903–910.
- [7] —, "SIC-free rate-splitting multiple access: Constellation-constrained optimization and application to large-scale systems," *arXiv preprint arXiv:2506.12668*, 2025.
- [8] M. Dai, B. Clerckx, D. Gesbert, and G. Caire, "A rate splitting strategy for massive mimo with imperfect CSIT," *IEEE Transactions on Wireless Communications*, vol. 15, no. 7, pp. 4611–4624, 2016.
- [9] Y. Mao, B. Clerckx, and V. O. Li, "Rate-splitting multiple access for downlink communication systems: bridging, generalizing, and outperforming SDMA and NOMA," *EURASIP J. Wireless Commun. Netw.*, no. 1, p. 133, May 2018.
- [10] R. Cerna Loli, O. Dizdar, B. Clerckx, and P. Popovski, "Hybrid automatic repeat request for downlink rate-splitting multiple access," *IEEE Transactions on Wireless Communications*, vol. 23, no. 10, pp. 15261–15274, 2024.
- [11] H. Joudeh and B. Clerckx, "Sum-rate maximization for linearly precoded downlink multiuser miso systems with partial CSIT: A rate-splitting approach," *IEEE Transactions on Communications*, vol. 64, no. 11, pp. 4847–4861, 2016.
- [12] Z. Li, C. Ye, Y. Cui, S. Yang, and S. Shamai, "Rate splitting for multi-antenna downlink: Precoder design and practical implementation," *IEEE Journal on Selected Areas in Communications*, vol. 38, no. 8, pp. 1910–1924, 2020.
- [13] Y. Xu, Y. Mao, O. Dizdar, and B. Clerckx, "Rate-splitting multiple access with finite blocklength for short-packet and low-latency downlink communications," *IEEE Transactions on Vehicular Technology*, vol. 71, no. 11, pp. 12333–12337, 2022.
- [14] Y. Wang, V. W. S. Wong, and J. Wang, "Flexible rate-splitting multiple access with finite blocklength," *IEEE Journal on Selected Areas in Communications*, vol. 41, no. 5, pp. 1398–1412, 2023.
- [15] C. E. Shannon, "A mathematical theory of communication," *The Bell System Technical Journal*, vol. 27, no. 3, pp. 379–423, 1948.
- [16] R. Gallager, "A simple derivation of the coding theorem and some applications," *IEEE Transactions on Information Theory*, vol. 11, no. 1, pp. 3–18, 1965.
- [17] N. Merhav, G. Kaplan, A. Lapidoth, and S. Shamai Shitz, "On information rates for mismatched decoders," *IEEE Transactions on Information Theory*, vol. 40, no. 6, pp. 1953–1967, 1994.
- [18] A. Lapidoth and P. Narayan, "Reliable communication under channel uncertainty," *IEEE Transactions on Information Theory*, vol. 44, no. 6, pp. 2148–2177, 1998.
- [19] J. Scarlett, A. G. i Fàbregas, A. Somekh-Baruch, and A. Martinez, "Information-theoretic foundations of mismatched decoding," *Foundations and Trends® in Communications and Information Theory*, vol. 17, no. 2–3, pp. 149–401, 2020. [Online]. Available: <http://dx.doi.org/10.1561/0100000101>
- [20] S. Zhang and B. Clerckx, "Optimal and suboptimal decoders under finite-alphabet interference: A mismatched decoding perspective," *arXiv preprint arXiv:2506.12646*, 2025.
- [21] S. Boyd and L. Vandenberghe, *Convex Optimization*. Cambridge University Press, 2004.
- [22] M. Chen, S. C. Liew, Z. Shao, and C. Kai, "Markov approximation for combinatorial network optimization," *IEEE Trans. Inf. Theory*, vol. 59, no. 10, pp. 6301–6327, Oct. 2013.
- [23] B. Clerckx, Y. Mao, R. Schober, and H. V. Poor, "Rate-splitting unifying SDMA, OMA, NOMA, and multicasting in MISO broadcast channel: A simple two-user rate analysis," *IEEE Wireless Communications Letters*, vol. 9, no. 3, pp. 349–353, 2020.
- [24] D.-S. Shiu, G. Foschini, M. Gans, and J. Kahn, "Fading correlation and its effect on the capacity of multielement antenna systems," *IEEE Transactions on Communications*, vol. 48, no. 3, pp. 502–513, 2000.
- [25] H. Joudeh and B. Clerckx, "Robust transmission in downlink multiuser miso systems: A rate-splitting approach," *IEEE Transactions on Signal Processing*, vol. 64, no. 23, pp. 6227–6242, 2016.
- [26] 3GPP, "3rd Generation Partnership Project; Technical Specification Group Radio Access Network; NR; Multiplexing and channel coding (Release 17)," 3GPP, Tech. Rep. TS 38.212 V18.6.0, Mar. 2025.